E27 Lab Report

Z0966990
L2 Electrical Engineering
January 21, 2017

Abstract

In this report, it is described how the MathWorks® Simulink® and SimScape™ graphical packages were used to model the way electrical and mechanical properties of a separately excited d.c. motor changed with respect to time. Using results from the simulation and the torque error term, it was shown the motor was capable of outputting enough torque to match the load at a range of different speeds.

Nomenclature

Acronyms

a.c.	Alternating current
d.c.	Direct current
e.m.f.	Electromotive force
r.p.m.	Revolutions per minute

Variables

B	Load torque constant	$\mathrm{N\,m\,s\,rad^{-1}}$
E	Motor back e.m.f.	V
I	Current	A
J	Moment of inertia	$\mathrm{kg\,m^2}$
K	Motor e.m.f. constant	$\mathrm{N\,m\,A^{-1}}$
		$\mathrm{V\,s\,rad^{-1}}$
L	Inductance	H
N	Motor speed	RPM
R	Resistance	Ω
T	Torque	$\mathrm{N\,m}$
V	Supply voltage	V
t	Time	s
ω	Motor speed	$\mathrm{rad\,s^{-1}}$

1 Introduction

Direct current motors are used in a variety of applications from power tools to electric vehicles. Unlike alternating current motors, a d.c. motor can be battery powered so are typically found in portable applications. However, precise torque and speed control is the primary benefit of d.c. motors over their a.c. counterparts. Motors driven by an alternating supply typically operate at a fixed frequency and speed, requiring a.c./a.c. convertors to change the supply frequency [1, p. 787].

As detailed in the remainder of the report, the speed of d.c. motors can be varied by changing the magnitude of the d.c. supply voltage, provided the motor can meet the loading requirements.

2 Background

According to Hughes in [1, p. 870], the most general form of d.c. motor is a separately excited d.c. motor, where the motor consists of two distinct parts—the stator field and armature—which each have their own independent d.c. voltage source. Under constant field operation, the magnetic field produced by current flowing through the field windings is unchanging. As current flows through windings in the armature, an electric field is produced which interacts with the static magnetic field. This interaction exerts an electromagnetic torque T_e on the armature, shown to be proportional to the armature current I_a as follows [1, p. 873]:

$$T_e = K I_a \;\Leftrightarrow\; I_a = \frac{T_e}{K} \tag{1}$$

The motor e.m.f. constant relates electromagnetic torque to armature current and is composed of the field current I_f and the coupling inductance between the field and stator windings L_{af}. According to [2], it is defined by the following:

$$K = L_{af} I_f \tag{2}$$

Figure 1 on the following page contains the circuit diagram of a separately excited d.c. motor subjected to a load torque T_L—based on the diagram given in [3]. When there is a net torque

on the armature the motor accelerates to some non-zero rotational speed. Consequently, the armature current moves relative to the stator field, so a back e.m.f. is induced across the armature windings such that it opposes its supply voltage in accordance with Faraday and Lenz's laws. Hughes shows the same motor constant from Equation 2 relates the back e.m.f. E to the rotational speed ω [1, p. 873].

$$E = K\omega \;\Leftrightarrow\; \omega = \frac{E}{K} \tag{3}$$

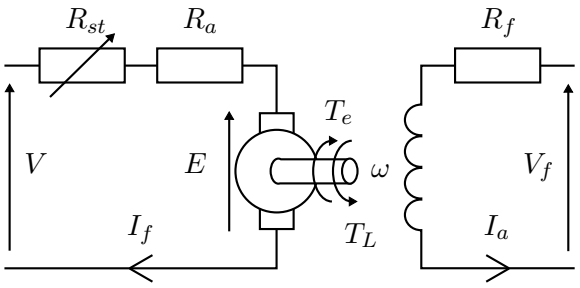

Figure 1: Circuit diagram of a seperately excited d.c. motor.

During the initial phase of operation, the rotational speed of the armature is small. As a result—according to Equation 3—the back e.m.f. is similarly small. As armature windings do not have a large resistance, this results in a potentially damaging current. To compensate, the starting resistance R_{st} in Figure 1 is set to some sufficiently large value to limit the current in the armature.

Applying Kirchoff's voltage law to the left hand side of Figure 1, an equation linking all the electrical properties of the armature is found:

$$E = V - I_a(R_a + R_{st}) \tag{4}$$

However, under normal operation after the motor has started, the resistance R_{st} is taken out of the armature to achieve a greater electromagnetic torque. The following equation describes how the electrical properties of the armature are related under normal operation and is the equation given by Hughes [1, p. 871]:

$$R_{st} = 0\ \Omega \;\Rightarrow\; E = V - I_a R_a \tag{5}$$

3 Methods

The Simulink package and SimScape library produced by MathWorks were used to model the behaviour of a d.c. motor system with a two step motor starter—using an implementation of TR-BDF2 developed in [4], [5]. In Simulink, TR-BDF2 is used in the ode23bt solving method. The block diagram of the model the solver was used on is documented in Figure 2 on the next page.

The d.c. machine was configured with the moment of inertia, resistance and inductance of the armature and field windings given in Table 1. The electrical inputs for these windings were implemented using external d.c. voltage sources; the magnitudes of which were also given in Table 1. For monitoring purposes, the output signals of the motor were armature current, field current, electromagnetic torque and speed.

Table 1: Defining parameters of d.c. motor system.

Armature Components			
V	Supply voltage	240	V
R_a	Armature resistance	1.6	Ω
L_a	Armature inductance	12	mH
J	Moment of inertia	0.5	$\mathrm{kg\,m^2}$
Field Components			
V_f	Field voltage	240	V
R_a	Field resistance	240	Ω
L_a	Field inductance	120	H
L_{af}	Coupling inductance	1.65	H
Load Characteristics			
T_{e0}	Initial torque	45	$\mathrm{N\,m}$
ω_0	Initial speed	1	$\mathrm{rad\,s^{-1}}$
B	Load constant*	0.247969	$\mathrm{N\,m\,s\,rad^{-1}}$

* See Equation 6 on the next page.

The d.c. machine was also configured with a starting field current as this would be constant throughout the simulation. Applying Ohm's

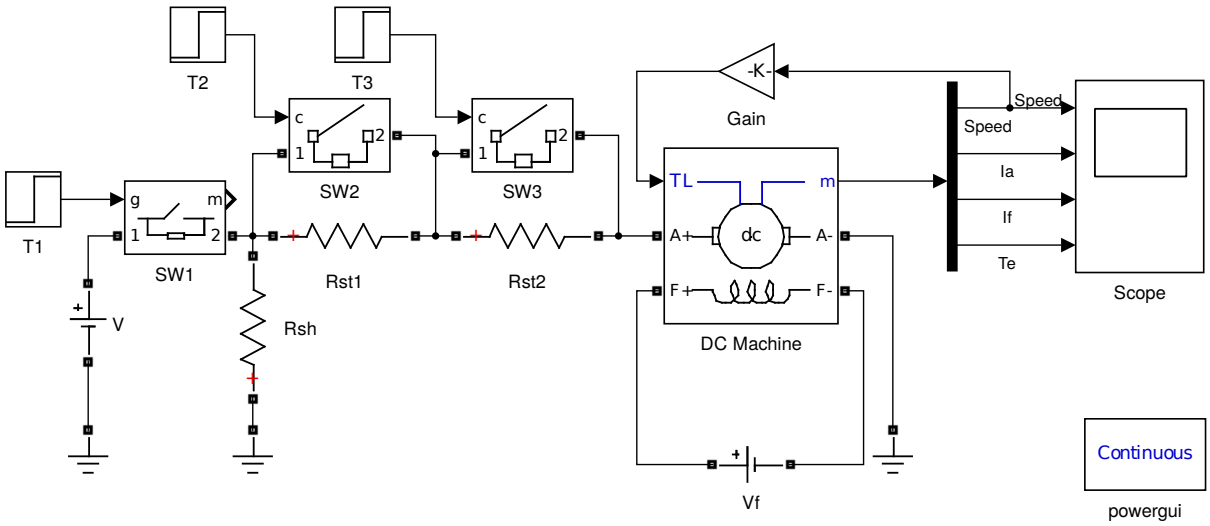

Figure 2: Block diagram of the Simulink model.

law to the right hand side of Figure 1, the stable field current was found:

$$I_f = \frac{V_f}{R_f}$$
$$I_f = \frac{240\ \text{V}}{240\ \Omega}$$
$$I_f = 1\ \text{A}$$

A constant useful for calculating additional model parameters was the motor e.m.f. constant; it's value was found by substituting the coupling inductance from Table 1 and the constant field current into Equation 2. The calculation yielded the following result:

$$K = L_{af} I_f$$
$$K = (1.65\ \text{H})(1\ \text{A})$$
$$K = 1.65\ \text{V s rad}^{-1}$$

Using the motor e.m.f. constant, the theoretical armature current at nominal speed can be calculated. The nominal speed given in [2] was 1220 RPM; this had to be converted into rad s^{-1}:

$$N = 1220\ \text{RPM} \Leftrightarrow \omega = 122\pi/3\ \text{rad s}^{-1}$$

Equation 3 was substituted into Equation 5 then rearranged to make I_a the subject. The armature current at nominal speed was found by plugging in values from Table 1 and the nominal speed calculated above, as follows:

$$K\omega = V - I_a R_a$$
$$\Leftrightarrow\ I_a = \frac{V - K\omega}{R_a}$$
$$I_a = \frac{240\ \text{V} - (1.65\ \text{V s rad}^{-1})(122\pi/3\ \text{rad s}^{-1})}{1.5\ \Omega}$$
$$I_a = 19.466\ \text{A}$$

3.1 Electric Hoist Load

The motor in the simulation was loaded with an electric hoist–type load. The rotational speed ω was used to described the load torque T_L using the following relationship:

$$T_L = B\omega \tag{6}$$

This was modelled by connecting the speed output of the d.c. machine to the torque load input via a constant gain block, configured with the multiplicative gain B given in Table 1. The topology of the network can be seen in the top-right of Figure 2.

3.2 Motor Starter

The motor starter in this model—represented as a variable resistor in Figure 1—was modelled using three switches in series with the armature winding. Two of the switches were parallel to a resistor, such that all current flowed through the resistor when the switch was open: when the switch was closed the current experienced no resistance. Figure 3 shows the circuit diagram of the network implemented, with the switches open as they were at the start of the simulation.

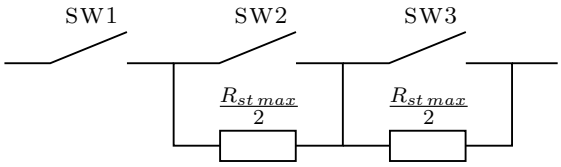

Figure 3: Circuit diagram of the motor starter used in the model.

An ideal switch was used to model SW1 and circuit breakers were used to model SW2 and SW3. These were closed at 0.5 s, 2.5 s and 3.5 s respectively using step blocks; this can be seen in Figure 2 on the previous page. The 0.5 s delay before powering the armature winding gave the field current and armature mechanics sufficient time to stabilise, whilst the other two switches removed the starting resistance in two steps.

The starting resistance limited the current flowing through the armature winding—to prevent damage—but the current had to be sufficiently large to generate the initial 45 N m of electromagnetic torque prescribed in Table 1.

The maximum allowable starting resistance $R_{st\,max}$ was calculated by substituting Equations 2 and 3 into Equation 4 and rearranging for R_{st}. The initial speed of the armature was assumed to be 1 rad s^{-1}. The result after substituting the necessary values was as follows:

$$\begin{aligned} K\omega &= V - \frac{T_e}{K}(R_a + R_{st}) \\ \Leftrightarrow\ R_{st} &= \frac{V - K\omega}{T_e/K} - R_a \\ R_{st\,max} &= \frac{240\ \text{V} - (1.65\ \text{V s rad}^{-1})(1\ \text{rad s}^{-1})}{(45\ \text{N m})/(1.65\ \text{N m A}^{-1})} \\ &\qquad - 1.5\ \Omega \\ R_{st\,max} &= 7.2395\ \Omega \end{aligned}$$

Each of the resistors marked Rst1 and Rst2 in the Figure 2 on the preceding page were configured with half the maximum allowable starting resistance: 3.6197 Ω.

3.3 Variable Speed Operation

The simulation model was also used to test the effectiveness of varying the speed of the motor by reducing the supply voltage. The target nominal speed was 800 RPM, which first had to be converted into rad s^{-1} before the new supply voltage could be found:

$$N = 800\ \text{RPM} \ \Leftrightarrow\ \omega = 80\pi/3\ \text{rad s}^{-1}$$

To achieve a speed of $80\pi/3$ rad s^{-1}, the motor would have to match load torque exerted by the electric hoist. The load torque at this speed was found by substituting the speed in rad s^{-1} into Equation 6 on the previous page as follows:

$$\begin{aligned} T_L &= B\omega \\ T_L &= (0.247969\ \text{N m s rad}^{-1})(80\pi/3\ \text{rad s}^{-1}) \\ T_L &= 20.774\ \text{N m} \end{aligned}$$

The armature current required to produce an equivalent amount of electromagnetic torque was found by substituting the load torque into

Equation 1, as follows:

$$\begin{aligned} I_a &= \frac{T_e}{K} \\ I_a &= \frac{20.774 \text{ N m}}{1.65 \text{ N m A}^{-1}} \\ I_a &= 12.590 \text{ A} \end{aligned}$$

Finally, the required supply voltage was found by substituting Equation 3 into Equation 5 and rearranging for V. The R_{st} term could be neglected, as at nominal speed the motor should have already started and stabilised.

$$\begin{aligned} K\omega &= V - I_a R_a \\ \Leftrightarrow\ V &= K\omega + I_a R_a \\ V &= (1.65 \text{ V s rad}^{-1})(80\pi/3 \text{ rad s}^{-1}) \\ &\qquad + (12.590 \text{ A})(1.5\ \Omega) \\ V &= 157.12 \text{ V} \end{aligned}$$

The d.c. voltage source for the armature winding was reconfigured with a magnitude of 157.12 V.

4 Results and Discussion

Figure 4 on the following page shows the evolution of the d.c. machine parameters during the 5 s simulation, performed at the original supply voltage of 240 V. Note the discontinuities at 0.5 s, 2.5 s and 3.5 s; when SW1, SW2 and SW3 were closed.

Those sudden increases in electromagnetic torque output can be attributed to the increases in armature current. Indeed, Equation 1 showed electromagnetic torque is directly proportional to the armature current.

As discussed in Section 3.2, when each of SW2 and SW3 were closed, the switch established a branch parallel with the resistor. The resistance of such a network is zero. Thus at 2.5 s and 3.5 s the starting resistance R_{st} decreased. Rearranging Equation 4 for I_a, it is clear the decrease in starting resistance was responsible for the sudden increase in armature current:

$$I_a = \frac{V - E}{R_a + R_{st}} \tag{7}$$

Equation 7 also explains why the torque decayed soon after each switch was closed. The armature had a rotational inertia of 0.5 kg m^2, so the armature speed lagged the net torque; this was evidenced in Figure 4—the rotational speed did not instantly change in reaction to the increase in electromagnetic torque. However, as the armature slowly accelerated, the back e.m.f. increased according to Equation 3. The increasing back e.m.f. reduced the current flowing through the armature and thus the torque decayed.

As the armature speed increased, electromagnetic torque decreased, but the load torque increased linearly—see Equation 6. The net torque $T_e - T_L$ driving the acceleration of the armature became smaller as the armature reached higher speeds. In Figure 4 this is apparent as the rate of change of armature speed became smaller as time progressed. Ideally, the net torque would be zero at the nominal speed: 1220 RPM $= 122\pi/3$ rad s^{-1} $= 127.76$ rad s^{-1}. Figure 4 suggests that by 5 s, the motor had reached nominal speed.

Figure 5 on the next page is the torque–speed plot for the simulation. Inspection of the load and electromagnetic torque traces suggest the torques converged at the nominal speed of 127.76 rad s^{-1}—the operating point where there was no net torque. The motor error term ΔT can be used to quantify the capability of the motor matching the full load torque at nominal speed. The error term is given by the following equation:

$$\Delta T = \frac{T_e - T_L}{T_{L\,max}} \tag{8}$$

Where T_e and T_L were recorded at 5 s and the full load torque $T_{L\,max}$ was calculated by substi-

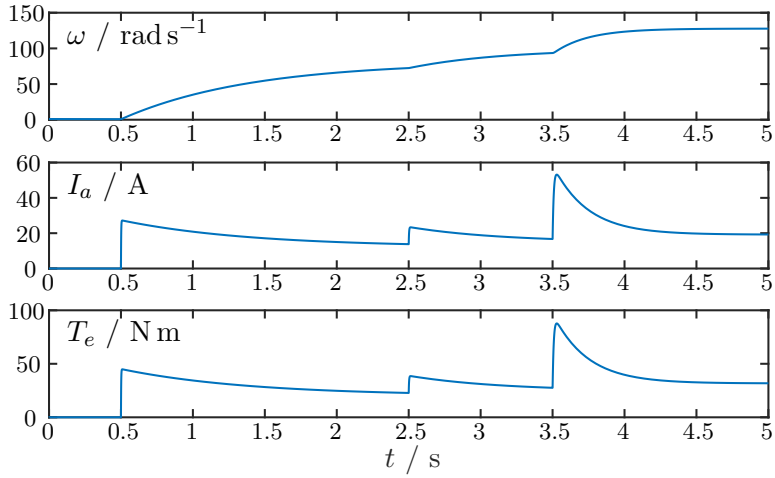

Figure 4: Simulated motor properties against time with 240 V supply.

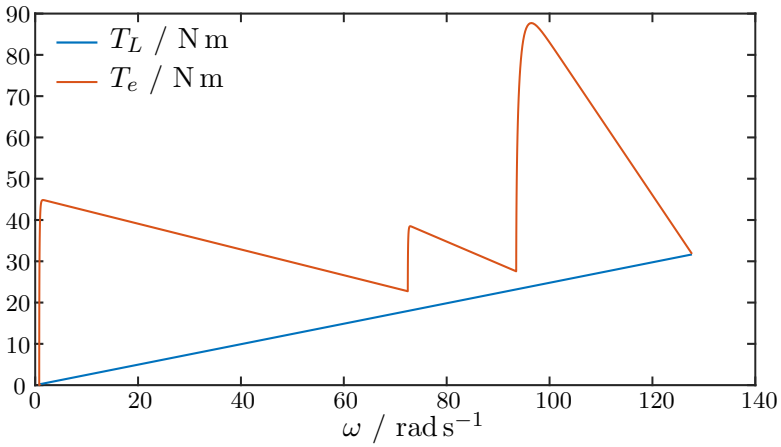

Figure 5: Torque–speed plot of simulation with 240 V supply.

tuting the nominal speed into Equation 6. From these values, the error term for the 1220 RPM simulation was computed using Equation 8 as follows:

$$\Delta T = \frac{T_e - T_L}{T_{L\,max}}$$
$$\Delta T = \frac{31.798\ \text{N m} - 31.664\ \text{N m}}{31.680\ \text{N m}}$$
$$\Delta T = 0.42333\%$$

Acceptable values for the error term are smaller than 1%, and indicate the motor was capable of matching the full load torque to within an acceptable degree of error. As the error term for this simulation was 0.42333%, the motor used in the simulation was successful at matching the full load torque. The error term was non-zero because the field winding inductance of 12 mH, whilst small, was also non-zero. The current would require an infinite amount of time to converge on a value where the load torque and electromagnetic torque match, so in practical applications error terms of zero are impossible.

Figure 6 on the following page shows the torque–speed plot for the simulation after the

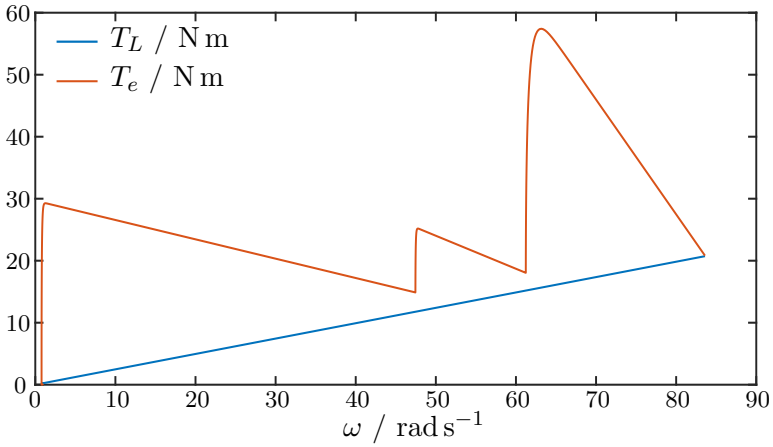

Figure 6: Torque–speed plot of simulation with reduced 157.12 V supply.

supply voltage had been reduced to 157.12 V in order to achieve a nominal speed of 800 RPM = $80\pi/3\,\mathrm{rad\,s^{-1}} = 83.776\,\mathrm{rad\,s^{-1}}$. Examining Figure 6, the load and electromagnetic torque appeared to converge at the nominal speed—the operating point; they converged in a similar manner to the torque–speed curves in Figure 5.

The error term was calculated as before:

$$\Delta T = \frac{T_e - T_L}{T_{L\,max}}$$
$$\Delta T = \frac{20.817\ \mathrm{N\,m} - 20.723\ \mathrm{N\,m}}{20.774\ \mathrm{N\,m}}$$
$$\Delta T = 0.42249\%$$

At the reduced speed, the motor was also capable of matching the full load torque to within an acceptable degree of error.

5 Conclusion

At low speeds, d.c. motors are susceptible to armature damage due to large currents. Whilst the motor starter resistance system was successful in reducing the armature current while starting the motor, the armature current still reached its peak value when the motor was accelerating up to nominal speed.

Varying the armature supply voltage was an effective method of varying the nominal speed of the d.c. motor. The motor used was capable of matching the target speeds of 1220 RPM at 240 V and 800 RPM at 157.12 V whilst meeting torque requirements of the electric hoist–type load specified to within an acceptable accuracy of 0.42333% and 0.42249% respectfully.

References

[1] E. Hughes, *Hughes electrical and electronic technology*, 10th ed. Pearson Education, 2010, pp. 787–873, ISBN: 9788131733660.

[2] K. Brigham, *Coursework: DC motor characteristics*, Durham University, Dec. 2016.

[3] B. Kazemtabrizi, *DC machines (3)*, Durham University, Feb. 2015.

[4] R. E. Bank, W. M. Coughran, W. Fichtner, E. H. Grosse, D. J. Rose, and R. K. Smith, "Transient simulation of silicon devices and circuits", *IEEE Transactions on Computer-Aided Design of Integrated Circuits and Systems*, vol. 4, no. 4, pp. 436–451, 1985.

[5] M. Hosea and L. Shampine, "Analysis and implementation of TR-BDF2", *Applied Numerical Mathematics*, vol. 20, no. 1, pp. 21–37, 1996.